Available online at www.sciencedirect.com

ScienceDirect

Energy Procedia 60 (2014) 166 – 172

Energy Procedia

E-MRS Spring Meeting 2014 Symposium Y "Advanced materials and characterization techniques for solar cells II", 26-30 May 2014, Lille, France

Investigation of the Structural, Optical and Electrical Properties of Cu_3BiS_3 Semiconducting Thin Films.

M.V. Yakushev[a,b]*, P. Maiello,[c] T. Raadik,[d] M.J Shaw,[a] P.R. Edwards,[a] J. Krustok,[d] A.V. Mudryi,[a,e] I. Forbes[c] and R.W. Martin[a]

[a]*Department of Physics, SUPA, University of Strathclyde, Glasgow, G4 0NG, UK*
[b]*URFU and Ural Branch of RAS, 620002 Ekaterinburg, Russia.*
[c]*Northumbria Photovoltaics Applications Centre, Northumbria University, Ellison Building, Newcastle upon Tyne NE1 8ST, UK*
[d]*Tallinn University Technology, Ehitajate tee 5, Tallinn 19086, Estonia*
[e]*Scientific-Practical Material Research Centre of the National Academy of Science of Belarus, P.Brovki 19, 220072 Minsk, Belarus*

Abstract

The elemental composition, structural, optical and electronic properties of *p*-type Cu_3BiS_3 thin films are investigated. The films are shown to be single phase orthorhombic, with a measured composition of $Cu_{3.00}Bi_{0.92}S_{3.02}$. A surface oxidation layer is also clarified using energy dependent X-ray microanalysis. Photoreflectance spectra demonstrate two band gaps (E_{gX} =1.24 eV and E_{gY} =1.53 eV at 4 K) associated with the X and Y valence sub-bands. The photocurrent excitation measurements suggest a direct allowed nature of E_{gX}. Photoluminescence spectra at 5 K reveal two broad emission bands at 0.84 and 0.99 eV quenching with an activation energy of 40 meV.

Peer-review under responsibility of The European Materials Research Society (E-MRS)

Keywords: Cu_3BiS_3, Thin films, Solar cells, Raman spectroscopy, Photoluminescence, Photoreflectance

*M.V. Yakushev. Tel.:+44-141-548-3374; fax: +44-141-552-2891.
E-mail address: michael.yakushev@strath.ac.uk

Peer-review under responsibility of The European Materials Research Society (E-MRS)
doi:10.1016/j.egypro.2014.12.359

1. Introduction

The compound semiconductors $Cu(InGa)Se_2$ and CdTe form the absorber regions in the best available single junction thin film photovoltaic (PV) cells [1]. They have demonstrated notable advances but there are issues with the high toxicity of tellurium (Te), cadmium (Cd) and selenium (Se) and also with large scale manufacture due to the limited supply of indium (In) and gallium (Ga), as well as Te and Se [2]. Ideally the large scale fabrication of thin film solar cells will involve development of PV technologies based on cheap, non-toxic elements which are abundant in the Earth's crust. This target drives the search for new semiconductor compounds, with high optical absorption coefficients matched to the solar spectrum, which are composed of low toxicity, low cost, earth abundant and easy to mine elements. The compound $Cu_2ZnSnSe_4$, referred to as CZTS, shows promise to match these requirements. CZTS can be viewed as a variation on $CuInSe_2$, where the rare and expensive In and Ga atoms are replaced with abundant and cheap Zn and Sn, on alternate In/Ga lattice sites [3,4]. Thin film solar cells fabricated using CZTS have demonstrated conversion efficiencies of over 12% [5]. However, the compound has a high degree of complexity and there is a very narrow single phase region in the phase diagram, leading to major challenges resulting from multiple secondary phases within the material [3]. This paper describes work on an alternative material containing bismuth (Bi), which is a non-toxic element whose reserves in the earth's crust are estimated to exceed those of In and Ga by two orders of magnitude. Considering ternary materials composed of Cu, S and Bi a very promising PV material is the natural mineral Cu_3BiS_3 (wittichenite), which has a very high absorption coefficient ($\sim 10^5$ cm^{-1}). There is, however, a wide spread of reported values for the band-gap, ranging from 1.14 to 1.41 eV [6,7,8,9]. Theoretical studies of this compound suggested an indirect band gap of 1.69 eV while the smallest direct band gap was estimated to be of 1.79 eV [10]. Cu_3BiS_3 has an orthorhombic crystal structure [6] and can be *p*-type doped [8,9]. A recent report has investigated of defect states and surface passivation of *p*-type Cu_3BiS_3 [8]. However the basic electronic properties vital for development of Cu_3BiS_3 photovoltaic devices are almost unexplored and there are no published studies of experimental work on the electronic band structure. The most common technique for bandgap measurement is optical absorption. However, multinary compounds can often have deep potential fluctuations [11] generating tails in the absorption spectra [12] and making analysis difficult such that the bandgap energy calculated from the absorption spectrum could be incorrect. Electro- or photoreflectance modulation methods [13] provide a more reliable method for measuring the bandgap.

In this paper we report the fabrication of thin films of Cu_3BiS_3 and characterization of their structural, optical and electronic properties.

2. Experimental details

The thin films of Cu_3BiS_3 were fabricated using a 2-stage process. Initially magnetron sputtering was used to deposit a 0.3 μm thick precursor layer of Cu and Bi on Mo-coated soda-lime glass, using 5N-purity elemental targets. Thermal evaporation was then used to coat this with a 1.5 μm thick film of 4N-purity sulphur. Subsequently this was heated for 30 min at 250 ^oC in an Ar atmosphere at a pressure of 1 mbar. The excess of sulphur is designed to ensure full conversion of the precursor layer during the heating process. Hot probe measurements were made immediately after fabrication of the film, demonstrating *p*-type conductivity. The surface morphology of the fabricated films was analysed using scanning electron microscopy (SEM) with wavelength-dispersive X-ray (WDX) microanalysis providing details of the elemental composition and homogeneity. X-ray diffraction (XRD) and Raman spectroscopy were used to investigate the structural properties of the films and the presence of secondary phases. The photoresponse was measured by immersing the films in a glass cell with 0.2 M aqueous solution of $Eu(NO_3)_3$, as an electron scavenging redox electrolyte, and illuminating with 75 Hz chopped monochromated light from a tungsten halogen lamp. A three electrode configuration was used with an Ag/AgCl reference electrode, a counter platinum electrode in addition to the molybdenum back contact. The photo-current was maximised by adjusting the potential with respect to the reference electrode. Photo-current excitation spectra were recorded using a standard Bentham lock-in amplifier and then normalised against calibrated silicon and germanium photodiodes, in order to correspond to apparent quantum efficiency (AQE). The photoreflectance (PR) measurements were carried out using a 40 cm focal length grating monochromator, Si detector and with the temperature varied in the range 10 to 300 K using a closed-cycle He cryostat. The primary beam comprised monochromated light from a 250 W halogen lamp and the secondary source was a solid state laser, emitting 80 mW of 405 nm light modulated at 85 Hz. Photoluminescence (PL) spectra were collected using

514 nm light from an Ar^+ excitation laser, with maximum power of 200 mW. A 1 m focal length grating monochromator and either an InGaAs photomultiplier tube (PMT) or a photodiode were used to detect PL in the spectral ranges from 0.9 to 1.7 μm and 0.9 to 1.9 μm, respectively. A closed-cycle He cryostat was used for temperature resolved measurements and a liquid helium cryostat for the excitation intensity dependent measurements.

3. Results and discussion

A secondary electron (SE) image of the surface of the CuBiS film is shown in Fig 1(a). The film is largely uniform and continuous. A higher resolution cross-sectional SE image is shown in Fig.1(b), demonstrates a dense homogeneous layer with an average thickness of 0.7 μm and grain size of 0.1 μm. The elemental composition of

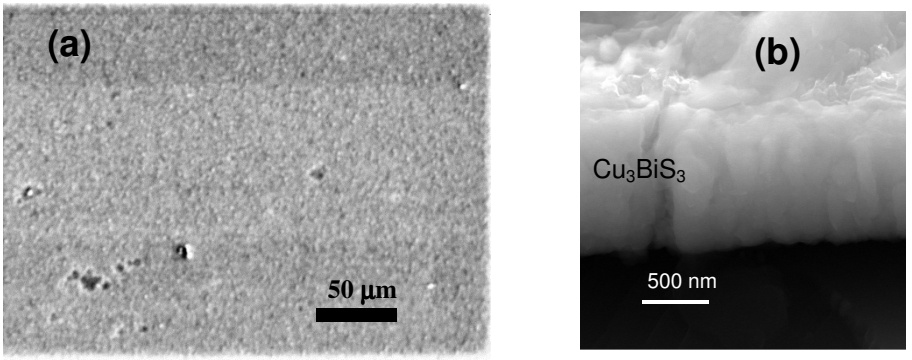

Fig.1. a) Secondary electron image of film surface. (b) Cross sectional SEM micrograph of Cu_3BiS_3/ Mo/ glass

the film was investigated using WDX analysis with an electron beam energy of 5 keV, which corresponds to a penetration depth of approximately 0.1 μm [14]. A thallium acid phthalate (TAP) crystal was used to measure the Cu Lα X-rays and a pentaerythritol (PET) crystal was used to measure Mα and Kα X-rays of Bi and S, respectively. A pseudocrystal was used to measure oxygen Kα. The standards used for quantitative measurements were pure Cu, pure Bi and pyrite (FeS_2). The elemental composition determined from averaging ten points along a 5 mm line was $Cu_{3.00}Bi_{0.92}S_{3.02}$. A good lateral homogeneity was observed, as shown in Fig.2(a). A low level of oxygen was also detected. Depth dependent WDX (Fig. 2(b)), using electron beam energies from 4 to 7 keV, demonstrate that this is due to surface oxidation with the oxygen signal decreasing linearly as the beam energy increases and the electrons penetrate further into the material.

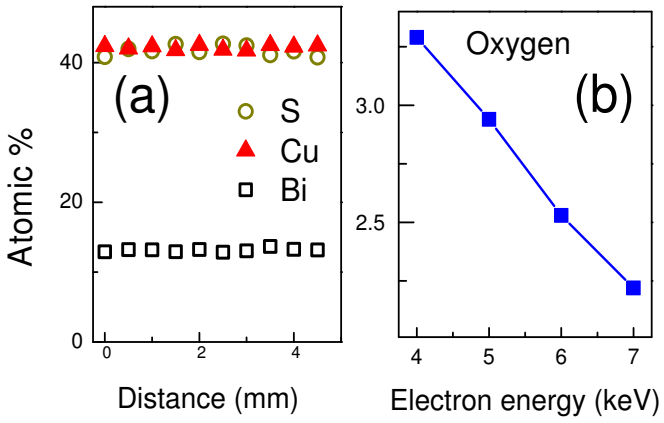

Fig.2. a) WDX data measured along a line across the film surface. (b) Depth dependent WDX data demonstrating that the oxygen is located at the surface

The XRD spectrum of the film shows a clear pattern of single phase orthorhombic lattice structure, as shown in Fig.3(a). A number of extra peaks, associated with metallic molybdenum and bismuth are also observed, indicating the presence of Bi clusters. Raman spectra, measured at different points of the films at room temperature, consistently reveal four modes at 96, 125, 264 and 292 cm^{-1} as shown in Fig. 3(b). The dominant peak at 292 cm^{-1} has a full width at half maximum (FWHM) of 12 cm^{-1}.

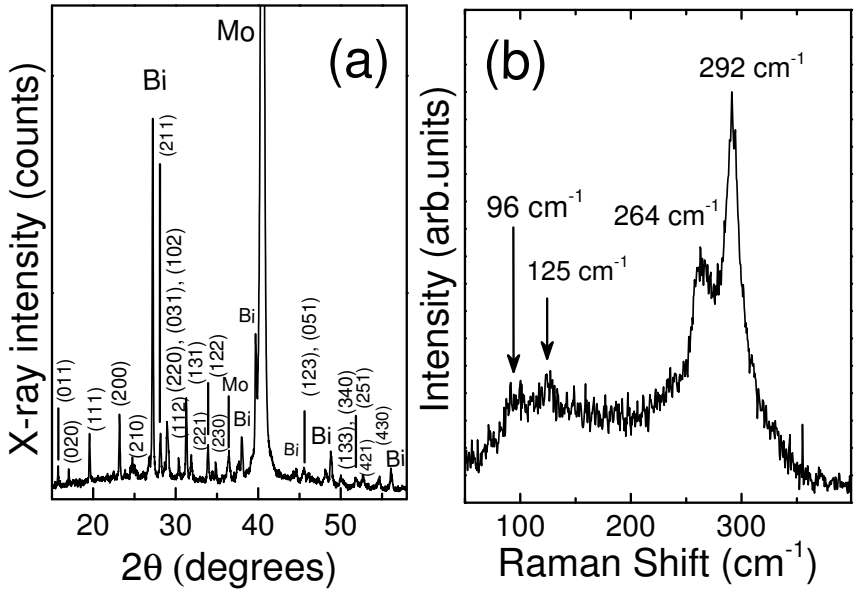

Fig.3. a) XRD pattern of Cu_3BiS_3/ Mo/ glass (b) Raman spectra of the Cu_3BiS_3 thin films

Photoreflectance data were used to measure the band gap of the Cu_3BiS_3 film. A modulation of the built-in electric field, created by the surface band bending due to the photo-injection of electron-hole pairs by a chopped incident laser beam, generates differential changes of the complex dielectric function and the amplitude of the PR signal $\Delta R/R$ [13]. Fig. 4(a) shows room temperature PR spectra, in which a strong resonance at 1.2 eV is seen. Decreasing the temperature down to 80 K shifts this resonance towards higher energies and reveals a second resonance at 1.5 eV. Further decrease of temperature, down to 10 K, shifts the resonances further towards higher energies and makes both resonances sharper. The experimental PR spectra were fitted with the function [15,16]:

$$\Delta R / R = \mathrm{Re}\left[\sum_{j=1}^{p} C_j e^{i\theta_j} (E - E_{g,j} + i\Gamma_j)^{-m}\right], \quad (1)$$

where E is photon energy, C_j, θ_j, $E_{g,j}$ and Γ_j are the amplitude, phase, transition energy and broadening parameter of each resonance, respectively, p is the number of resonances and i is imaginary unit. A two resonance (p=2) fit was used. The m parameter is defined by the type of the critical point and m = 5/2, corresponding to interband transitions and a three-dimensional critical point, has been assumed for the calculations. The fitted curves for the temperature 10, 80 and 300 K are shown by solid lines in Fig. 4(a). Values for E_g for different temperatures, determined using the best fits, are shown in Fig.4(b). The presence of two band gaps can be associated with a splitting of the valence band, as has been reported for ternary I-III-IV_2 semiconductor compounds with a chalcopyrite structure [17,18]. Measurements on two different phases, chalcopyrite and orthorhombic, of one of these compounds ($AgInS_2$), reveals a splitting of the valence band into three sub-bands for both of them [19]. In the chalcopyrite phase the splitting into A, B and C sub-bands occurs due to the simultaneous influence of the crystal field and spin orbit interaction whereas in the orthorhombic one a splitting into X, Y and Z

sub-bands is considered to be solely due to the influence of the crystal field. For the orthorhombic structure of Cu_3BiS_3 we use the notations X and Y for the top two bands. The temperature dependencies of E_{gX} and E_{gY} were fitted with the expression introduced by O'Donnell and Chen [20]:

$$E_g(T) = E_g(0) - S < h\nu > / \left[\coth(< h\nu >/2kT) - 1\right], \quad (2)$$

where $E_g(0)$ is the band gap energy at 0 K, S is a dimensionless coupling constant and $< h\nu >$ represents an average phonon energy.

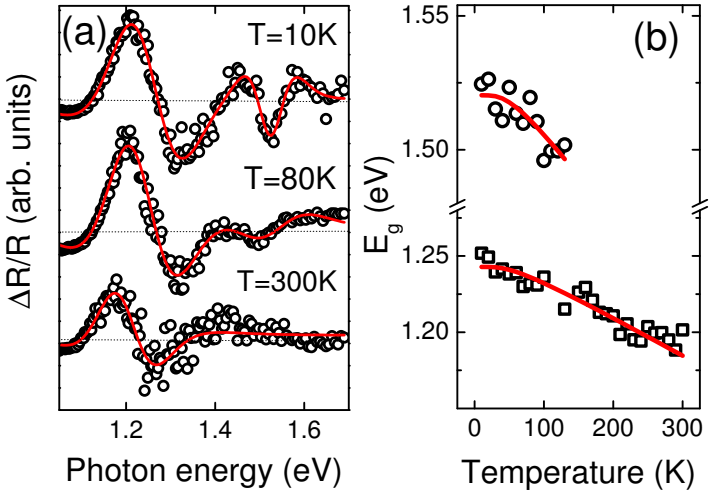

Fig. 4. (a) PR spectra of Cu_3BiS_3 films at different temperatures with best fits (solid lines) using Eq.(1), (b) temperature dependence of the X and Y band gap energies with best fits (solid lines) using Eq.(2).

The solid curves in Fig 4(b) are the best fits of the $E_g(T)$ values using equation (2) with the fitting parameters shown in Table 1. The average phonon energies are in the range of the measured energies of the Raman modes. Fig.4(b) demonstrates a strong decrease of both energy gaps with increasing temperature as well as a reduction in the splitting of the valence bands, from 0.28 eV at 10 K to 0.27 eV at 100 K.

Table 1. The band gap E_g, coupling constant S and average phonon energy $<h\nu>$ for the X and Y valence bands, determined by fitting the experimental temperature dependencies of E_g using equation (2).

Valence band	$E_g(0)$ (eV)	S	$<h\nu>$(meV)
X	1.24	0.54	6
Y	1.53	0.70	20

Fig. 5(a,b) shows PL spectra, which provide information on the mechanisms of radiative recombination and the nature of defects. The low temperature (4.2 K) PL spectra in Fig.5(a), measured with the extended range photodiode and PMT, contain two non- resolved broad bands: A1 at about 0.99 eV with a full width at half maximum (FWHM) of 160 meV and (A2) at 0.84 eV with FWHM of 140 meV. The relative intensities of the bands vary at different points on the sample, but their spectral positions remain the same. The dependence of the total integrated PL intensity (I) of both bands with increasing laser power P was fitted to the equation $I \sim P^{\gamma}$. A value of $\gamma \approx 0.71$ is determined, suggesting that these bands are associated with defect related transitions [21]. No significant spectral shifts were observed as the excitation laser power density was increased from 0.26 to 2 W/cm^2. The PL intensity of the A1 band increases at a greater rate than that of the A2 band, as clearly seen in Fig.5(a) which shows spectra

excited with laser power densities of 0.26, 0.78 and 2 W/cm^2 and normalized to the A2 band intensity for 2 W/cm^2. The low energy tail of the A2 band is cut-off beyond the 1.7 μm limit of the PMT used for this measurement. The temperature dependence of the PL spectra from 5 to 90 K is shown in Fig.5(b). These spectra reveal significant water absorption at 0.9 eV. The spectral positions of the A1 and A2 bands do not shift in energy within this temperature range. Also the A1 band is seen to quench at a greater rate than A2.

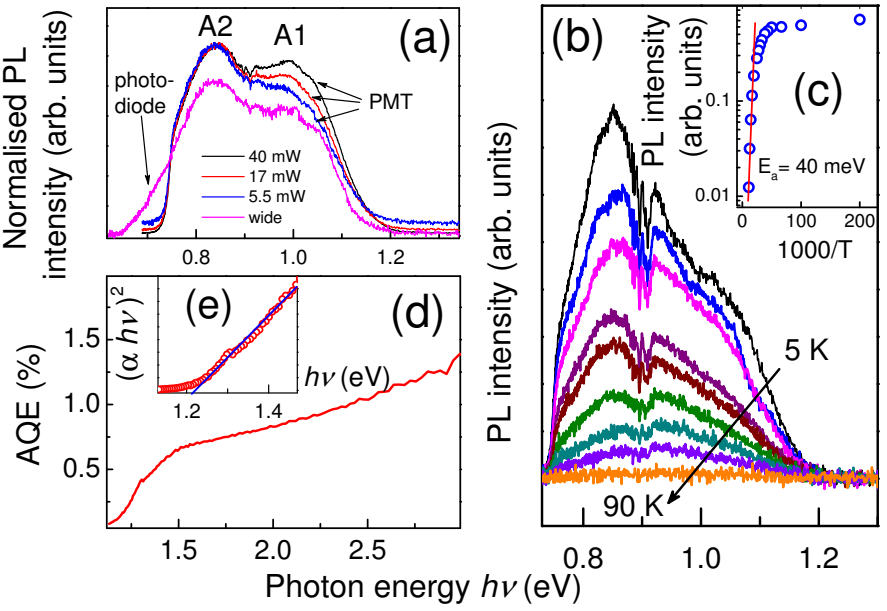

Fig.5. Normalised PL spectra at different laser excitation power (a), temperature dependence of the PL spectra (b), Arrhenius plot of the temperature quenching of the A1 and A2 band integrated intensity (○ experimental points, - fitted straight line) (c). Apparent quantum efficiency of the Cu_3BiS_3 film (a), the dependence of $[\alpha h\nu]^2$ on $h\nu$ and estimation of E_g (d).

An Arrhenius plot of the temperature quenching for the integrated intensity of both bands I is shown in Fig. 5(c), revealing a straight line region between 50 and 90 K. The best fit of the experimental data points in this region was achieved assuming a model with one recombination channel:

$$I(T)=I_0(1+A\exp(-E_a/kT) \quad (3)$$

where I_0 (intensity at the lowest temperature), E_a (activation energy) and A are fitting parameters and k is the Boltzmann constant. An activation energy of 40 ± 4 meV is determined. Thus the observed temperature quenching of both bands can be caused by ionization of a shallower defect, located at 40 meV from the valence or conduction band.

An *AQE* spectrum, shown in Fig.5(d), demonstrates a photoresponse of about 1 % in the photon range of 1.1 - 2.3 eV. A similar photoresponse also measured using the Eu^{+3} electrolyte has been reported in [9]. Varying the potential with respect to the reference electrode the authors of [9] derived the doping density values. The *AQE* depends on absorption coefficient α as [22], $AQE = 1- \exp(-\alpha W)$, where W is the width of the space charge region. For a direct allowed transition, the dependence of the absorption coefficient on the photon energy $h\nu$ should follow the relation, $\alpha h\nu \propto (h\nu - E_g)^{1/2}$. Fig.5(e) demonstrates a clear linearity of the $[h\nu\ ln(1-AQE)]^2$ dependence on $h\nu$ suggesting a direct allowed nature of the band gap in Cu_3BiS_3. Extending this line to the intersection with the $h\nu$ – axis, as shown in Fig.5(e), gives an estimate of E_g = 1.22 eV which is close to that determined from PR measurements at room temperature.

Conclusion

In conclusion, the properties of Cu_3BiS_3 films have been extensively investigated. Photo-reflectivity at 10 K reveals two band gaps, at 1.24 and 1.53 eV, which were associated with the X and Y valence sub-bands respectively. Two broad bands were observed in low temperature PL spectra at 0.99 and 0.84 eV. Their excitation power dependencies revealed no spectral shifts but a redistribution of PL intensity towards the higher energy band. Both bands were quenching at temperatures of 90 K.

Acknowledgement

This work was supported by the EPSRC (SUPERGEN II "PV21", EP/F029624/2 and EP/H5 0009X/1), BCFR (F13IC-018), the US Civilian Research & Development Foundation (CRDF Global) and the Ural Branch of RAS (RUE2-7105-EK-13), RFBR (14-02-00080, 13-03-96032, 12-U3-1006), Estonian Science Foundation Grant G9369.

References

[1] Green MA, Emery K, Hishikawa Y, Warta W. Solar cell efficiency tables (version 37). Prog Photovolt Res Appl 2011; 19: 84-9.
[2] Andersson BA. Materials availability for large-scale thin-film photovoltaics. Prog Photovolt Res Appl 2000; 8: 61-16.
[3] Siebentritt S, Schorr S. Kesterites - a challenging material for solar cells. Prog Photovoltaics 2012; 20: 512-8.
[4] Luckert F, Hamilton DI, Yakushev MV, Beattie N, Zoppi G, Moynihan M, Forbes I, Karotki AV, Mudryi AV, Grossberg M, Krustok J, Martin RW. Optical properties of high quality $Cu_2ZnSnSe_4$ thin films. Appl Phys Lett 2011; 99: 0621041 -3.
[5] Wang W, Winkler MT , Gunawan O , Gokmen T , Todorov TK , Zhu Y ,Mitzi DB, Device Characteristics of CZTSSe Thin-Film Solar Cells with 12.6% Efficiency 2013; Adv. Energy Mater. 4: 1301465
[6] Estrella V, Nair MTS, Nair PK. Semiconducting Cu_3BiS_3 thin films formed by the solid-state reaction of CuS and bismuth thin films. Semicond Sci Technol 2003;18: 190-5.
[7] Yakushev MV, Maiello P, Raadik T, Shaw MJ, Edwards PR, Krustok J, Mudryi AV, Forbes I, Martin RW, Influence of Chemical Composition inhomogeneity on Spatial position of fundamental absorption edge of $Cu(In,Ga)Se_2$ solid solutions Thin Solid Films 2014; 562: 195
[8] Mesa F, Gordillo G. Effect of preparation conditions on the properties of Cu_3BiS_3 thin films grown by a two – step process. J Phys: Conf. Series 2009; 167: 0120191-5.
[9] Colombara D, Peter LM, Hutchings K, Rogers KD, Schäfer S, Dufton JTR, Islam MS. Formation of Cu_3BiS_3 thin films via sulfurization of Bi-Cu metal precursors. Thin Solid Films 2012; 520: 5165-7.
[10] Kumar M, Persson C. Cu_3BiS_3 as a potential photovoltaic absorber with high optical efficiency. Appl Phys Let 2013; 102: 062109-3.
[11] Krustok J, Collan H, Yakushev M, Hjelt K. The role of spatial potential fluctuations in the shape of the PL bands of multinary semiconductor compounds. Phys Scr 1999; T79: 179-4.
[12] Dirnstorfer I, Hofmann M, Lampert MD, Karg F, Meyer BK. $CuIn(Ga)Se_2$ solar cells: Characterization of the absorber material. Inst Phys Conf Ser 1998; 152: 233-4.
[13] Pollak FH, Shen H. Modulation spectroscopy of semiconductors: bulk/thin film, microstructures, surfaces/interfaces and devices. Mater Sci Eng 1993; R10: 275-10.
[14] Martin RW, Edwards PR, O'Donnell KP, Mackay EG, Watson IM, Micro-composition and luminescence of InGaN emitters. phys. stat. sol. (a) 2002; 192: 117
[15] Aspnes DE, in: Balkanski M (Ed.), *Handbook on Semiconductors II,* North-Holland, Amsterdam, 1980, Vol. 2, Chap. 4A, p.109 - 365.
[16] Raadik T, Krustok J, Yakushev MV. Photoreflectance study of $AgGaTe_2$ single crystals. Physica B: Physics of Condensed Matter 2011; 406: 418 - 3.
[17] Yakushev MV, Luckert F, Faugeras C, Karotki AV, Mudryi AV, Martin RW. Diamagnetic shift of the A free exciton in $CuGaSe_2$, Appl Phys Lett 2010; 97: 1521101-3.
[18] Shay JL, Wernick JH. Ternary Chalcopyrite Semiconductors-Growth, Electronic Properties, and Applications. Oxford: Pergamon Press; 1975.
[19] Shay JL, Tell B, Schiavone LM, Kasper HM, Thiel F. Energy bands of $AgInS_2$ in the chalcopyrite and orthorhombic structures. Phys Rev B 1974; 9: 1719–5.
[20] K.P. O'Donnell and X. Chen, Temperature dependence of semiconductor band gaps, Appl. Phys. Lett. 58 (1991) 2924 - 2926.
[21] Schmidt T, Lischka K, Zulehner W. Excitation-power dependence of the near-band-edge photoluminescence of semiconductors. Phys Rev B 1992; 45: 8989 - 6.
[22] Scragg J, Dale PJ, Peter LM, Zoppi G, Forbes I. New routes to sustainable photovoltaics: evaluation of Cu_2ZnSnS_4 as an alternative absorbermaterial. phys stat sol (b) 2008; 245: 1772-7.